Session 3: Properties of high-mass protostars

Excursion to Etna

Excursion to Etna

Hypercompact HII regions

Stan Kurtz

Centro de Radioastronomía y Astrofísica, UNAM, Morelia, Michoacán, Mexico
email: s.kurtz@astrosmo.unam.mx

Abstract. The physical parameters of HII regions span orders of magnitude in scale. The classes most closely linked to star formation are the smallest, densest, and, presumably, youngest stages: compact, ultracompact, and hypercompact HII regions.

Although hypercompact HII regions have been known for over ten years, until recently only a very small number of these regions were known. Moreover, it is only in the past several years that these regions have come to be recognized as a distinct class of HII region and that attempts have been made to understand their place in the scheme of massive star formation.

Here we present a summary of the observational studies to date. We give special emphasis to radio continuum studies, which indicate density gradients within the ionized gas, and to radio spectral line studies, which show unusually broad recombination line profiles. Possible interpretations of these aspects of hypercompact HII regions are discussed, and their implications for the interpretation of hypercompact HII regions as an evolutionary stage in the high-mass star formation process.

Keywords. stars: formation, (ISM:) HII regions

---

1. Introduction

The first hypercompact (HC) HII region was discovered by Gaume *et al.* (1995) near the NGC 7538 ultracompact (UC) HII region. At the time, a half-dozen surveys had been made, and hundreds of UC HII regions were already known (see Table 1). So why did the HC HII regions escape notice for so long? One possibility, of course, is that they are very rare. Throughout most of the 1980's, for example, only a handful of UC HII regions were known. Not until the pioneering survey of Wood & Churchwell (1989) did the field explode, with their discovery of some 75 UC HII regions — far more than the number expected given the dynamical lifetime (see Rodríguez, this volume). Another possibility, however, is that the UC HII region surveys, including Wood & Churchwell (1989) and others that followed, suffered from an observational bias that made HC HII regions difficult to detect.

Table 1 summarizes the main ultracompact HII region surveys made to date. It is clear that with the exception of the De Pree *et al.* (2005) survey (which was restricted to the Sgr B2 and W49 regions) all the existing surveys were at moderate centimeter wavelengths, with 6 cm (5 GHz) being a typical value. This characteristic wavelength of $\lambda \sim 6$ cm implies an observational bias toward HII regions with densities a few times 10^4 cm^{-3}. This was a "feature not a bug" of the ultracompact surveys, because they were looking for regions with sizes of about 0.1 pc and densities of order 10^4 cm^{-3} — i.e., regions smaller and denser than the typical compact HII regions that had been known for over a decade.

To see why this frequency implies an observational bias (and what we might do to remedy the matter) it's useful to review the thermal bremsstrahlung spectrum of a classical (spherical, uniform, isothermal) HII region (see Figure 1). The turnover frequency, at which the optical depth $\tau = 1$, divides the optically thick from the optically thin

Table 1. Surveys of Ultracompact HII Regions

Survey	Year	Approximate Source Count	Wavelengths (cm)
Wood & Churchwell	1989	75	2, 6
Garay *et al.*	1993	16	2, 6, 20
Kurtz *et al.*	1994	75	2, 4
Miralles *et al.*	1994	12	2, 6
Becker *et al.*	1994	450	6, 20
Walsh *et al.*	1998	100	3.5, 4.5
Giveon *et al.*	2005	280	6, 20
De Pree *et al.*	2005	100	1.3, 0.7

regime of the spectrum. The flux density of the HII region peaks at slightly higher frequencies than the turnover; at lower frequencies the flux density drops as the square of the frequency, at higher frequencies the flux density drops very slowly with frequency, as $\nu^{-0.1}$.

The problem is immediately evident from an approximate expression for the optical depth of thermal bremsstrahlung emission (Mezger & Henderson, 1967):

$$\tau_\nu \approx 0.082 \; T_e^{-1.35} \, \nu^{-2.1} \int n_e^2 \, ds. \qquad (1.1)$$

An immediate implication of this relation is that for emission measures greater than 4×10^9 pc cm^{-6}, the turnover frequency for optically thin emission will be at 30 GHz (1 cm) or higher. Such high emission measure HII regions are optically thick at centimeter wavelengths and have flux densities falling as the square of the observation frequency.

Put a different way, setting $\tau = 1$ in equation 1.1 and solving for the turnover frequency gives

$$\nu_t \approx \left[0.082 \; T_e^{-1.35} \int n_e^2 \, ds \right]^{0.476} \qquad (1.2)$$

Because the electron density term of the emission measure is first squared, and later raised to the 0.476 power, the turnover frequency is essentially linear in the density.

A turnover frequency of 5 GHz ($\lambda = 6$ cm) corresponds to an emission measure of nearly 10^8 pc cm^{-6} (9×10^7, to be precise). For a UC HII region with a nominal size of 0.1 pc, this corresponds to electron densities of about 3×10^4 cm^{-3}. But now imagine a population of HII regions 10 times smaller ($d \sim 10$ mpc) and 30 times denser ($n_e \sim 10^6$ cm^{-3}). Their emission measures would be of order 10^{10} pc cm^{-6}, resulting in a turnover frequency of about 50 GHz, or $\lambda = 6$ *milli*meters, rather than 6 *centi*meters. Such an HII region would be in the optically thick regime of its spectrum at 6 cm, and hence the flux density could be as much as $100\times$ lower than it's near-peak value at 6 mm! This is indicated by the dashed curve in Figure 1. Most of the UC HII surveys were snap-shot observations with detection limits at the milliJansky level. Hence, there could be a population of small, dense, optically thick HII regions, with peak millimeter flux densities of order 100 mJy, that was completely missed by these surveys. Just such a situation is illustrated for the source G75.78+0.34 in Figure 2.
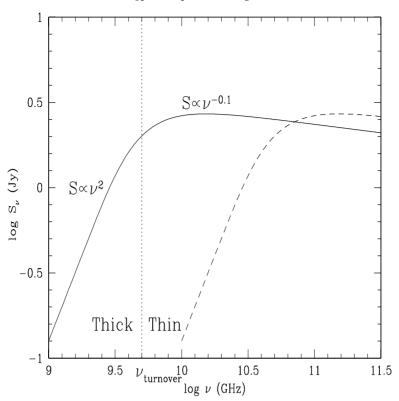
Figure 1. Radio spectrum of thermal bremsstrahlung emission from a spherical, homogeneous, isothermal HII region. The turnover frequency, shown by the vertical dashed line, corresponds to 5 GHz or $\lambda = 6$ cm. The spectral index assumes intermediate values for frequencies near the turnover. At lower frequencies the ionized gas is optically thick, and the radio emission is proportional to ν^2; at higher frequencies the gas is optically thin, and the emission is proportional to $\nu^{-0.1}$. The dashed line shows the spectrum of an HII region with the same peak flux density, but with an emission measure 100 times higher; resulting in a turnover frequency that is 10 times higher. Such an HII region, if observed at 6 cm, would present a flux density 100 times lower its low emission measure counterpart

2. The Spectra of Hypercompact HII Regions

The radio spectrum of G75.78 is shown in Figure 3. There are several notable features to this spectrum. First, the spectral index of $+1.4$ is less than then nominal value of $+2$, indicating a density gradient within the ionized gas (see Franco *et al.* (2000) and Rodríguez, this volume). Second, there does not appear to be a turnover in the free-free spectrum. If the turnover frequency actually is above the highest frequency point (at 230 GHz), this would imply an emission measure in excess of 2×10^{11} pc cm^{-6}, resulting in an electron density greater than 6×10^6 cm^{-3}. We note in passing that this is quite similar to the 10^7 cm^{-3} densities found in hot molecular cores, thought to be the birth sites of massive stars (Kurtz *et al.* 2000). There is a suggestion that the radio spectrum is flattening at 7 mm, in which case one might be tempted to interpret the 3 mm and 1 mm flux densities as arising from warm dust. Although plausible, this interpretation would then be forced to explain the extremely low spectral index of $\sim +1.3$ for the dust emission, for which values $\sim +3$ are far more typical.

If the 3 mm and 1 mm flux densities do arise from ionized gas rather than warm dust, we are left with the third notable feature of this spectrum: the apparent lack of dust
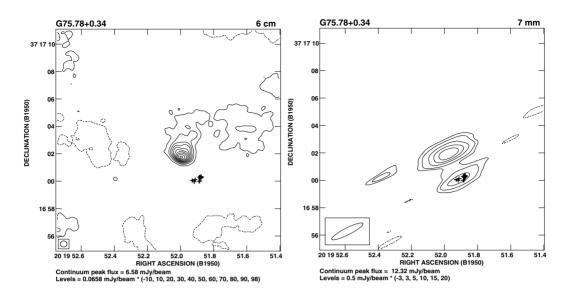
Figure 2. Continuum images of the G75.78+0.34 UC and HC HII regions. At left is the 6 cm image from Wood & Churchwell (1989). The crosses indicate water masers, from Hofner & Churchwell (1996). No continuum emission is seen from this position at centimeter wavelengths. At right is the same sky area, imaged at 7 mm. Continuum emission from the HC HII is clearly detected, coincident with the water maser position. From Carral *et al.* (1997).

emission. Typically (though not always!) the 1 mm flux density of a UC HII region will be 1–2 orders of magnitude higher than the centimeter continuum. *If* the 1 mm flux density reflects the free-free continuum, then we are left with the puzzle of why there isn't a substantial dust contribution at this wavelength.

Although the spectrum of G75.78 suggests the absence of dust, this should not be taken to mean that dust is not actually present. If the dust were particularly hot, for example, it's emission curve would be pushed to higher frequencies. Alternatively, if the dust emission arises from a much larger region than the free-free emission, then the interferometric observations at 1 and 3 mm may resolve out the dust emission. A conspiracy of density gradients in the ionized gas and temperature gradients in the dust might also result in a spectrum similar to the one shown. The final interpretation of the spectrum in Figure 3 is yet to be made. But regardless of what this interpretation may be, we note that the spectrum shown here has several remarkable differences from virtually all UC HII region spectra.

3. The Radio Recombination Lines of Hypercompact HII Regions

Once a significant sample of HC HII region candidates came to be recognized, it was quickly noticed that there was a remarkable overlap between the HC HII candidates and the so-called *broad-line regions*, which present unusually wide radio recombination lines Johnson, De Pree, & Goss 1998. The known broad-line regions are indicated in Table 2; with the exception of one source (G25.5+0.2) all sources on the list are also candidate HC HII regions.

UC HII regions typically show radio recombination line (RRL) widths of 30–40 km s^{-1}. As noted in the table, candidate HC HII regions show substantially broader line profiles.
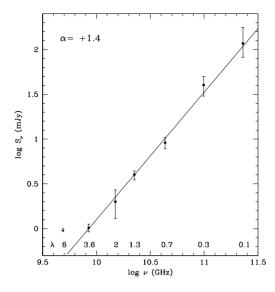
Figure 3. Spectrum of the G75.78+0.34 hypercompact HII region. The source was not detected by the 6 cm observations of the Wood & Churchwell (1989) UC HII region survey. Subsequent VLA and OVRO observations detect the hypercompact component from 3.6 cm to 1 mm. The interpretation of the spectrum is not clear, but it is consistent with free-free emission from a very high emission measure object.

Table 2. Broad-line Regions

Source	RRL	FWHM (km s^{-1})	Dist (kpc)	Reference
NGC 7538	H66α	180	3.0	1
G25.5+0.2	H42α	161	14.5	2
Sgr B2	H66α	80	8.5	3
W49 AA	H66α	50	11.4	4
W49 AB	H66α	60	11.4	4
W49 AG	H66α	45	11.4	4
M17-UC1	H52α	47	2.2	5
G28.2−0.0	H92α	74	9.1	6

a Table is adapted from Johnson *et al.* 1998. References are: 1, Gaume *et al.* 1995; 2, Shepherd *et al.* 1995; 3, De Pree *et al.* 1996; 4, De Pree *et al.* 1997, 2004; 5, Johnson *et al.* 1998; 6, Sewilo *et al.* 2004.

An example is shown in Figure 4. The northern, hypercompact source, has a linewidth of 75 km s^{-1} while the southern, ultracompact source, has a linewidth of 35 km s^{-1}.

There are three possible causes for these unusually broad recombination lines. In high density regions, pressure broadening can be a significant factor — particularly for highly excited transitions, which are extremely sensitive to this effect. Another possible cause is bulk motions within the gas — either infall, outflow, or rotation. Finally, unresolved, multiple sources might give rise to the broader profiles, either from locally higher densities, relative motion of the sources, or a combination of the two. High resolution RRL observations will be crucial to determine the contribution of the different mechanisms. Figure 5 shows a high resolution image of the northern, hypercompact component of
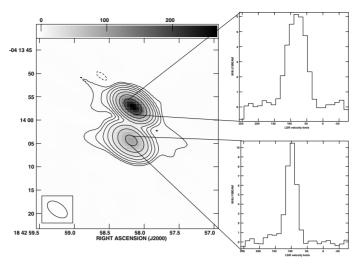
Figure 4. The continuum image on the left shows the G28.2−0.0 "binary" UCHII region. At the right are shown the H92α line profiles from the central region of each component. The northern, hypercompact source has a FWHM of 75 km s^{-1} while the southern, ultracompact source has a FWHM of 35 km s^{-1} (Sewilo *et al.* 2004).

Table 3. Physical Parameters of HII Regions

Class of Region	Size (pc)	Density (cm^{-3})	Emis. Meas. (pc cm^{-6})	Ionized Mass (M$_\odot$)
Hypercompact	$\lesssim 0.03$	$\gtrsim 10^6$	$\gtrsim 10^{10}$	$\sim 10^{-3}$
Ultracompact	$\lesssim 0.1$	$\gtrsim 10^4$	$\gtrsim 10^7$	$\sim 10^{-2}$
Compact	$\lesssim 0.5$	$\gtrsim 5\times 10^3$	$\gtrsim 10^7$	~ 1
Classical	~ 10	~ 100	$\sim 10^2$	$\sim 10^5$
Giant	~ 100	~ 30	$\sim 5 \times 10^5$	10^3–10^6
Supergiant	>100	~ 10	$\sim 10^5$	10^6–10^8

G28.2−0.0. The line profiles show significant variation at distinct positions within the shell-like structure (see the poster by Sewilo *et al.* in this volume). Whatever the final interpretation of the broad RRL profiles, it will clearly be a factor which distinguishes hypercompact from ultracompact regions.

4. Theoretical Developments

4.1. *Spectra*

A significant step toward understanding the radio spectra of both ultracompact and hypercompact HII regions has been made by Ignace & Churchwell (2004). They modeled HII regions as an ensemble of clumps of varying optical depths. Their models were able to reproduce the intermediate values of the spectral indices seen in both ultra and hypercompact regions. Moreover, the models were able to reproduce these intermediate indices over exceptionally broad frequency ranges, as observed in hypercompact regions. Although RRL were beyond the scope of their work, it is quite possible that this model
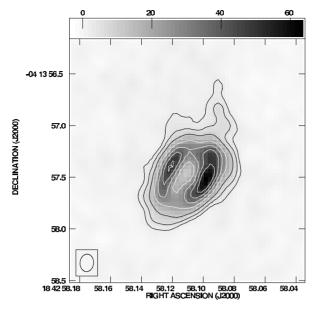
Figure 5. A high resolution (0.15 arcsecond) continuum image of the northern, hypercompact component of G28.2−0.0 shown in Figure 4 (from the poster by Sewilo *et al.* this volume). Significant variations are seen in the H92α line profile across the face of this shell-like source. High spatial resolution radio recombination lines will be essential to determine the nature of the line-broadening in these objects.

can also reproduce the broad RRL profiles observed in HC HII regions. There is significant potential in this model, and hopefully it will be further developed in the near future.

4.2. *Photoevaporating Disks*

Photoevaporating accretion disks around massive stars (Hollenbach *et al.* 1994; Lizano *et al.* 1996) were originally proposed to explain the smallest UC HII regions, and typically those with rising radio spectra. The radio emission region in their model (see Figure 6) has a characteristic size scale of $r_g = GM_*/a^2 \approx 10^{15}M_{10}$ cm, or about 1 mpc for a 30 M$_\odot$ star. The radio emission would arise from a region roughly 5–10 times larger than r_g, which corresponds well to the sizes of HC HII regions. The disk wind would present a density gradient, which could explain the spectral indices seen. Although not explored by Hollenbach *et al.* 1994 or Lizano *et al.* 1996, the disk/wind dynamics might give rise to broad recombination line profiles. Although this model was proposed over 10 years ago, it has tremendous potential for application to HC HII regions; it sorely needs to be revisited in this context (see Lizano, this volume).

4.3. *Inflow/Outflow Models*

Two models have been proposed to confine the ionized gas of the HII region to hypercompact sizes by considering accretion toward the protostellar object (Tan & McKee 2003; Keto 2003). Ironically, the models act by completely opposite mechanisms to confine the gas. Tan & McKee propose that the high outflow rates resulting from *high* accretion rates will produce small, jet-like hypercompact HII regions. Keto proposes that *low* accretion rates, with the material passing through a small ionized region where stellar gravity dominates thermal pressure, can produce long-lived, hypercompact HII regions. Both models predict broad recombination line profiles.
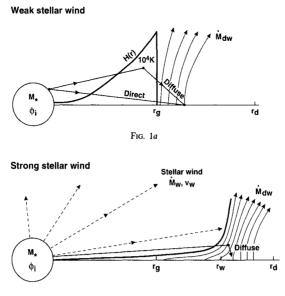
Figure 6. A schematic diagram of the two cases of the photo-evaporating disk model. From Hollenbach *et al.* 1994. In this model the radio emission would come from a region several times larger than the gravitational radius, r_g, which for a 30 M$_\odot$ star would be about 1 mpc.

A thorough discussion of these two models is clearly beyond the scope of this brief presentation. What is clear, however, is that observational tests of the models will be challenging. In particular, angular resolutions of order 50 milli-arcseconds (10 mpc at 5 kpc) will be required to resolve the source structures. Such high angular resolutions imply VLA observations. To distinguish the affects of pressure-broadening from bulk motions of the gas will require observations of millimeter recombination lines such as H40α and H30α. Such high frequencies imply millimeter arrays, which lack the necessary high angular resolution. The Sub-Millimeter Array can make important contributions in the short term; clearly ALMA will be the instrument to definitively address this issue.

5. Conclusions

By way of conclusion, it is perhaps worth asking just where the sequence compact $\rightarrow$ ultracompact $\rightarrow$ hypercompact, will end. Will some even smaller, denser HII region emerge? Or have we reached the end of the line? The answer to this question may also bear on whether we should think of these three classes of objects as being merely smaller and denser versions of the same thing or whether there is something intrinsically different about each class.

Definitive answers to these questions are not yet clear. But we can find significant guidance from the size scales of the different classes. In particular, compact and ultracompact HII regions, with typical dimensions of 0.5 and 0.1 pc, respectively, are of the scale of OB clusters. The Orion Trapezium cluster, for example, has a size of about 0.16 pc. To within a factor of 2 or 3, such a cluster (with all the associated objects) might be found within either a compact or an ultracompact HII region. Hypercompact HII regions, with sizes of about 0.03 pc (6,000 AU) or smaller, begin to push this limit. At some point, not too far beyond the nominal 30 mpc size, one will encounter characteristic size scales for single star (or binary star) formation. As such, hypercompact HII regions (or possibly one further step beyond them) will of necessity constitute the ionized gas around a single

stellar system, as opposed to a massive star cluster, as would be expected for compact and ultracompact HII regions.

Acknowledgements

References

Becker, R. H., White, R. L., Helfand, D. J., & Zoonematkermani, S. 1994, *Astrophys. J. Supp.* 91, 347

Carral, P., Kurtz, S. E., Rodríguez, L. F., De Pree, C. G., & Hofner, P. 1997, *Astrophys. J.* 486, L103

De Pree, C. G., Gaume, R. A., Goss, W. M., & Claussen, M. J. 1996, *Astrophys. J.* 464, 788

De Pree, C. G., Mehringer, D. M., & Goss, W. M. 1997, *Astrophys. J.* 482, 307

De Pree, C. G., Wilner, D. J., Deblasio, J., Mercer, A. J., & Davis, L. E. 2005, *Astrophys. J.* 624, L101

De Pree, C. G., Wilner, D. J., Mercer, A. J., Davis, L. E., Goss, W. M., & Kurtz, S. 2004, *Astrophys. J.* 600, 286

Franco, J., Kurtz, S., Hofner, P., Testi, L., García-Segura, G., & Martos, M. 2000, *Astrophys. J.* 542, L143

Garay, G., Rodríguez, L. F., Moran, J. M., & Churchwell, E. 1993, *Astrophys. J.* 418, 368

Gaume, R. A., Goss, W. M., Dickel, H. R., Wilson, T. L., & Johnston, K. J. 1995 *Astrophys. J.* 438, 776

Giveon, U., Becker, R. J., Helfand, D. J., & White, R. L. 2005, *Astron. J.*, 129, 348

Hofner, P., & Churchwell, E. 1996, A&AS, 120, 283

Hollenbach, D., Johnstone, D., Lizano, S., & Shu, F. 1994, *Astrophys. J.* 428, 654

Ignace, R. & Churchwell, E. 2004, *Astrophys. J.* 610, 351

Johnson, C. O., De Pree, C. G., & Goss, W. M. 1998, *Astrophys. J.* 500, 302

Keto, E. 2003, *Astrophys. J.* 599, 1196

Kurtz, S., Cesaroni, R., Churchwell, E., Hofner, P., & Walmsley, C. M. 2000, *Protostars and Planets IV*, Ed. V. Mannings, A. P. Boss, & S. S. Russell, (Tucson: University of Arizona Press), p. 299

Kurtz, S., Churchwell, E., & Wood, D. O. S. 1994, *Astrophys. J. Supp.* 91, 659

Lizano, S., Cantó, J., Garay, G., & Hollenbach, D. 1996, *Astrophys. J.* 468, 739

Mezger, P. G., & Henderson, A. P. 1967, *Astrophys. J.* 147, 471

Miralles, M. P., Rodríguez, L. F., & Scalise, E. 1994, *Astrophys. J. Supp.* 92, 173

Sewilo, M., Churchwell, E., Kurtz, S., Goss, W. M., & Hofner, P. 2004, *Astrophys. J.* 605, 285

Shepherd, D. S., Churchwell, E., & Goss, W. M. 1995, *Astrophys. J.* 448, 426

Tan, J. C., & McKee, C. F. 2003, *ASP Conference Series* 221, also astro-ph/0309139

Walsh, A. J., Burton, M. G., Hyland, A. R., & Robinson, G. 1998, *M.N.R.A.S.*, 301, 640

Wood, D. O. S., & Churchwell, E. 1989, *Astrophys. J. Supp.* 69, 831